Article:
Roberts, Adam, Nagar, Rupa, Brandt, Cordelia et al. (2022) The Leishmania donovani Ortholog of the Glycosylphosphatidylinositol Anchor Biosynthesis Cofactor PBN1 Is Essential for Host Infection. MBio. e00433-22. ISSN: 2150-7511

https://doi.org/10.1128/mbio.00433-22

AMERICAN SOCIETY FOR MICROBIOLOGY | mBio®

RESEARCH ARTICLE

The *Leishmania donovani* Ortholog of the Glycosylphosphatidylinositol Anchor Biosynthesis Cofactor PBN1 Is Essential for Host Infection

Adam Roberts,[a,b] Rupa Nagar,[c] Cordelia Brandt,[d] Katherine Harcourt,[d] Simon Clare,[d] Michael A. J. Ferguson,[c] Gavin J. Wright[a,b]

[a]Cell Surface Signalling Laboratory, Wellcome Sanger Institute, Hinxton, Cambridge, United Kingdom
[b]Department of Biology, Hull York Medical School, York Biomedical Research Institute, University of York, York, United Kingdom
[c]Wellcome Centre for Anti-Infectives Research, School of Life Sciences, University of Dundee, Dundee, United Kingdom
[d]Pathogen Support Team, Wellcome Sanger Institute, Hinxton, Cambridge, United Kingdom

ABSTRACT Visceral leishmaniasis is a deadly infectious disease caused by *Leishmania donovani*, a kinetoplastid parasite for which no licensed vaccine is available. To identify potential vaccine candidates, we systematically identified genes encoding putative cell surface and secreted proteins essential for parasite viability and host infection. We identified a protein encoded by *LdBPK_061160* which, when ablated, resulted in a remarkable increase in parasite adhesion to tissue culture flasks. Here, we show that this phenotype is caused by the loss of glycosylphosphatidylinositol (GPI)-anchored surface molecules and that *LdBPK_061160* encodes a noncatalytic component of the *L. donovani* GPI-mannosyltransferase I (GPI-MT I) complex. GPI-anchored surface molecules were rescued in the *LdBPK_061160* mutant by the ectopic expression of both human genes *PIG-X* and *PIG-M*, but neither gene could complement the phenotype alone. From further sequence comparisons, we conclude that *LdBPK_061160* is the functional orthologue of yeast *PBN1* and mammalian *PIG-X*, which encode the noncatalytic subunits of their respective GPI-MT I complexes, and we assign *LdBPK_061160* as *LdPBN1*. The *LdPBN1* mutants could not establish a visceral infection in mice, a phenotype that was rescued by constitutive expression of *LdPBN1*. Although mice infected with the null mutant did not develop an infection, exposure to these parasites provided significant protection against subsequent infection with a virulent strain. In summary, we have identified the orthologue of the PBN1/PIG-X noncatalytic subunit of GPI-MT I in trypanosomatids, shown that it is essential for infection in a murine model of visceral leishmaniasis, and demonstrated that the *LdPBN1* mutant shows promise for the development of an attenuated live vaccine.

IMPORTANCE Visceral leishmaniasis is a deadly infectious disease caused by the parasites *Leishmania donovani* and *Leishmania infantum*. It remains a major global health problem, and there is no licensed highly effective vaccine. Molecules that are displayed on the surface of parasites are involved in host-parasite interactions and have important roles in immune evasion, making vaccine development difficult. One major way in which parasite surface molecules are tethered to the surface is via glycophosphatidylinositol (GPI) anchors; however, the enzymes required for all the biosynthetic steps in these parasites are not known. Here, we identified the enzyme required for an essential step in the GPI anchor-biosynthetic pathway in *L. donovani*, and we show that while parasites lacking this gene are viable *in vitro*, they are unable to establish infections in mice, a property we show can be exploited to develop a live genetically attenuated parasite vaccine.

KEYWORDS glycophosphatidylinositol biosynthesis, parasitology, mass spectrometry, leishmaniasis, enzyme, bioluminescence

Editor Yung-Fu Chang, College of Veterinary Medicine, Cornell University

Address correspondence to Gavin J. Wright, gavin.wright@york.ac.uk.

The authors declare no conflict of interest.

Received 15 February 2022
Accepted 7 March 2022

Leishmania sp. parasites are estimated to infect up to 1 million individuals every year, with the vast majority of infections concentrated in low- and middle-income countries (1). Clinically, human leishmaniasis presents itself in either cutaneous, mucocutaneous, or visceral form, with the cutaneous form being responsible for the majority of cases and the more deadly visceral form having a fatality rate of up to 7% in areas where the disease is endemic (2). Leishmaniasis is currently treated with drugs that include amphotericin B, miltefosine, and antimonials; however, these drugs exhibit toxicity and teratogenicity, and the associated side effects make compliance with effective dosing regimens difficult (3). Importantly, there are reports that the parasite has evolved resistance to these drugs, leading to increased incidences of treatment failure (4–6). While drug screening and repurposing strategies are providing a new source of safe and effective antileishmanial compounds for assessment in the clinic (7–9), the need to continually treat new infections and the poor patient access to medical infrastructures in the regions of the world where leishmaniasis is endemic mean that an effective vaccine would be a valuable control tool for this disease.

Because of their direct accessibility to the host humoral immune response, proteins that are displayed on the surface of pathogens are often excellent vaccine candidates. One way that eukaryotic organisms attach proteins to the plasma membrane is to covalently couple polypeptides to a glycosylphosphatidylinositol (GPI) anchor. GPI anchors are attached to the C-terminal amino acid α-carboxyl group by an amide bond to the ethanolamine (EtN) residue of a conserved GPI anchor core structure of EtN-*P*-6Manα1-2Manα1-6Manα1-4GlcNα1-6*myo*-inositol-1-*P*-lipid, where the lipid can be phosphatidylinositol (PI) or inositol phosphoceramide (IPC). The conserved GPI anchor core structure can be substituted with sugar and nonsugar substituents in a species- and/or cell type-specific manner. The PI or IPC component is embedded in the outer leaflet of the plasma membrane, thus affording stable membrane association (10, 11). The synthesis of the core structure begins by the transfer of an α-linked *N*-acetylglucosamine (GlcNAc) to the inositol ring on the cytoplasmic side of the endoplasmic reticulum (ER) followed by de-N-acetylation to create GlcN-PI. This molecule is then "flipped" into the lumenal-facing leaflet of the ER membrane, where three α-linked mannose residues are added by the sequential activity of three distinct GPI mannosyltransferases (GPI-MT-I, -II, and -III) using dolichol-phosphate mannose as the donor substrate (10, 11). Following further processing, including the addition of the EtN-*P* group from the phospholipid phosphatidylethanolamine (PE), the GPI anchor replaces a C-terminal hydrophobic polypeptide sequence on the target protein in a transamidase reaction catalyzed in the ER by a GPI-transamidase enzyme complex (11).

The cell surfaces of parasitic protozoa, and especially kinetoplastids, are characterized by highly abundant proteins that are attached to the plasma membrane by GPI anchors and/or by GPI anchor-like glycoinositolphospholipids (GIPLs) and/or large (phospho)oligosaccharides attached to GPI anchor-like structures (10). The structural hallmark of all GPI and GPI-like structures is the motif Manα1-4GlcNα1-6*myo*-inositol-1-*P*-lipid, and type 1 GPIs include the protein GPI anchors and are defined by the sequence Manα1-6Manα1-4GlcNα1-6*myo*-inositol-1-*P*-lipid, whereas some GIPLs are type 2 GPIs with Manα1-3Manα1-4GlcNα1-6*myo*-inositol-1-*P*-lipid sequences [or hybrid GPIs with branched (Manα1-3)Manα1-6Manα1-4GlcNα1-6*myo*-inositol-1-*P*-lipid sequences]. The large (phospho)oligosaccharide containing structures are generally attached to type 2 GPI structures. Such molecules have long been associated with immune evasion, immune modulation, and host and vector cell interactions, and these include the highly abundant allelically expressed variant surface glycoprotein (VSG) of African trypanosomes (12, 13), the *Leishmania* spp. lipophosphoglycans (LPGs) (14), and the GP63 surface protease of *Leishmania* sp. parasites (15).

Several independent studies have demonstrated that GPI-anchored molecules are important virulence factors or required for transmission (16, 17). The biosynthetic pathway for protein GPI anchors was largely delineated in protists using cell-free lysates of

Trypanosoma brucei (18) and forward genetics in *Saccharomyces cerevisiae* (19); in mammals, many enzymes were discovered by expression complementation cloning in chemically induced mutant CHO cells, for example (20, 21). The variations leading to the type II and hybrid GPI structures were determined in *Leishmania* spp. (10). While the core structure of the protein GPI anchor is well conserved between mammals and kinetoplastid parasites, there are differences in their assembly (11). For example, in contrast to mammals, in trypanosomes, the first mannose is added to GlcN-PI, which lacks inositol acylation (20, 22). These differences have the potential to be exploited to develop new antiparasitic drugs (23, 24) and also mean that identifying the direct functional orthologs for some of the biosynthetic enzymes based on sequence identity alone can be difficult. One example of this is the protein orthologous to mammalian PIG-X/yeast PBN1 (25, 26), which acts as a cofactor for the catalytic subunit of GPI mannosyltransferase 1 (PIG-M/GPI14) and which has so far eluded identification in kinetoplastid parasites by sequence similarity searching.

Here, we demonstrate that the protein encoded by the gene *LdBPK_061160* is the PIG-X/PBN1 functional homolog of the trypanosomatids. We show that while parasites lacking this protein are viable *in vitro*, it is required for patent host infection.

RESULTS

Parasites lacking LdBPK_061160 have an increased adhesion phenotype due to the loss of GPI-anchored surface molecules. By systematically targeting genes encoding predicted cell surface and secreted proteins in *Leishmania donovani* using CRISPR/Cas9 technology, we previously identified a gene encoding a typical type I membrane protein, LdBPK_061160, which, when disrupted, caused a striking increase of parasite adhesion to the tissue culture flask plastic (Fig. 1A and B). It is known that the surface of procyclic promastigote stage *Leishmania* spp. parasites are dominated by GPI-linked molecules, including LPG, GIPLs and a protease (GP63) (14, 27), and so we asked if there were any major changes in the surface abundance of these molecules. By staining parasites with specific antibodies, we demonstrated complete ablation of LPG and GP63 on the surface of mutant parasites compared to the parental strain (Fig. 1C and D). Importantly, correct localization could be fully restored by constitutively expressing *LdBPK_061160*, demonstrating that this effect was specific to this gene and not attributable to off-target Cas9 activity (Fig. 1C and D). It has been suggested that these abundant parasite surface molecules may act as a steric shield, preventing the binding of host proteins, including antibodies, to the cell surface (28). Indeed, by contrast to the parental line, we observed that mutant parasites were brightly stained with antibodies present in convalescent-phase serum from chronically infected mice, confirming the loss of a protective glycocalyx (Fig. 1E). This increased antibody staining observed in the mutant was distributed across the whole cell surface, rather than being restricted to a particular region (Fig. 1F). Together, these data demonstrate an important role for *LdBPK_061160* in the presentation of GPI-anchored molecules at the surface.

Loss of *LdBPK_061160* leads to the accumulation of GlcN-PI, the substrate of the GPI-MT I complex. To characterize the function of *LdBPK_061160* in more detail, we first hypothesized that it may have a role in GPI anchor biosynthesis. To establish this, the lipid extracts from the parental, *LdBPK_061160*$^{-/-}$ mutant, and genetically rescued parasites were analyzed using negative-ion electrospray mass spectrometry (ES-MS) and molecular species confirmed by mass spectrometry of fragment ions (ES-MS^2). The ES-MS data revealed the accumulation of a molecular species consistent with GlcN-PI in the *LdBPK_061160* null mutant, $[M - H]^-$ ions at *m/z* 984.64 and *m/z* 1,012.67 (Fig. 2A). By contrast, the parental and genetically rescued cell lines both showed undetectable levels of these putative GlcN-PI species (Fig. 2B and C). The identities of the two putative GlcN-PI species were confirmed by ES-MS^2 (Fig. 2D to F), with the observed difference in precursor masses a result of varying alkyl chain length at the *sn-1* position ($C_{16:0}$ and $C_{18:0}$ for *m/z* 984.64 and *m/z* 1,012.67, respectively). At the *sn-2* position, both precursors were found to have the same acyl chain (stearic acid,

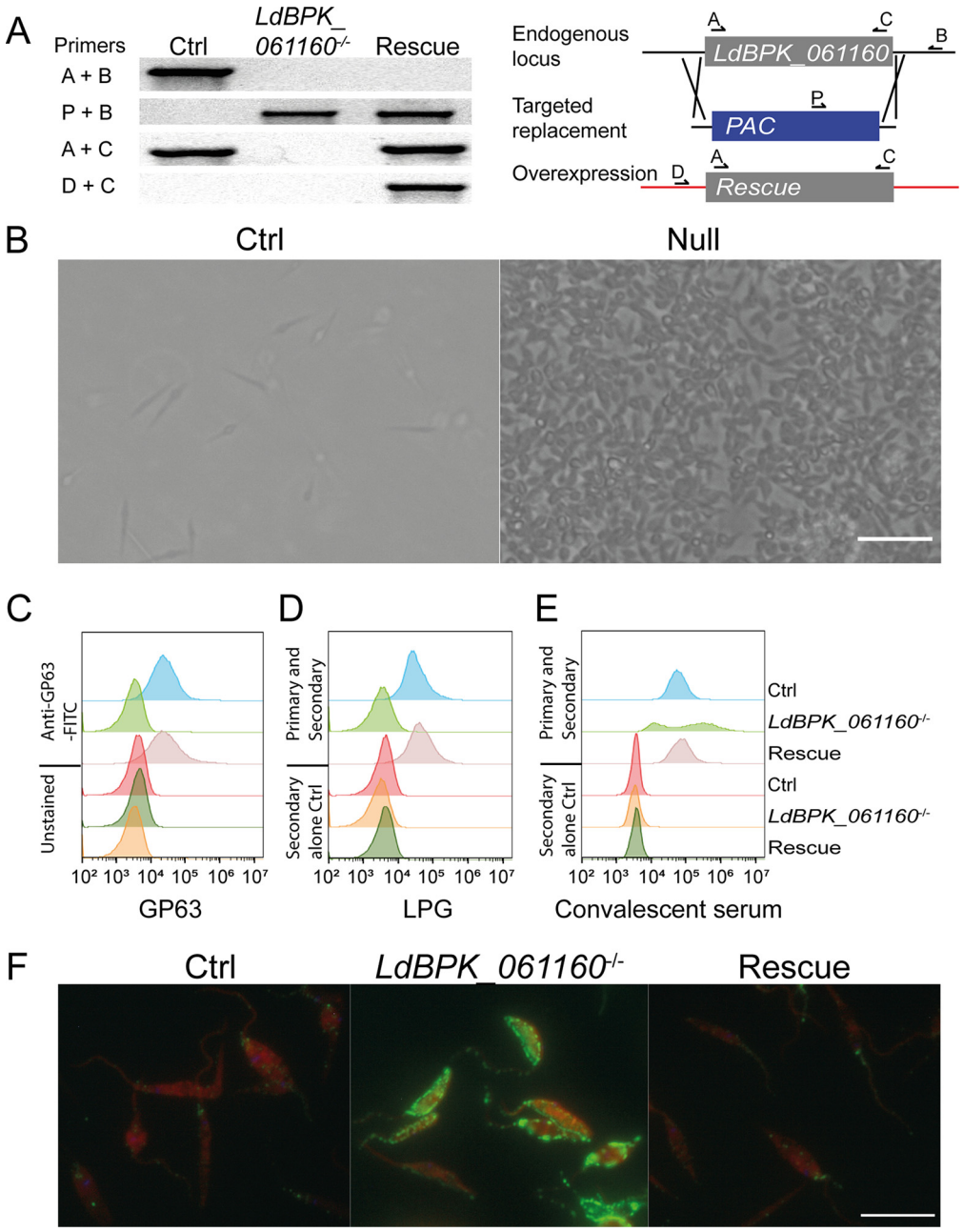

FIG 1 Genetic targeting of *LdBPK_061160* caused a cellular adhesion phenotype due to the catastrophic loss of cell surface GPI-anchored molecules. (A) Diagnostic PCRs demonstrating genetic targeting of *LdBPK_061160* locus. Schematic of the endogenous locus showing location and orientations of diagnostic primers and PCR products which demonstrate targeted replacement and ectopic overexpression of *LdBPK_061160* in the null mutant with genetic rescue from a nonendogenous locus. (B) Procyclic promastigote stage *L. donovani* parasites lacking *LdBPK_061160* exhibit increased adherence to tissue culture flasks (right) compared to the parental control (left). Bar, 20 μm. (C and D) Mutant parasites showed complete loss of cell surface GPI-anchored molecules as measured by flow cytometry, including GP63 (C) and LPG (D), compared to the parental control (Ctrl). In both panels C and D, surface expression was fully rescued by overexpression of *LdBPK_061160* (Rescue). (E) Parasites lacking *LdBPK_061160* were more brightly stained with convalescent-phase serum from chronically infected mice than the parental control, an effect that was rescued by expression of *LdBPK_061160*. (F) Images of the parasites analyzed for panel E showing that the epitopes recognized by chronically infected serum were distributed over the entire cell surface of the promastigote-stage *L. donovani* parasites. A representative image from two independent experiments is shown. Bar, 15 μm.

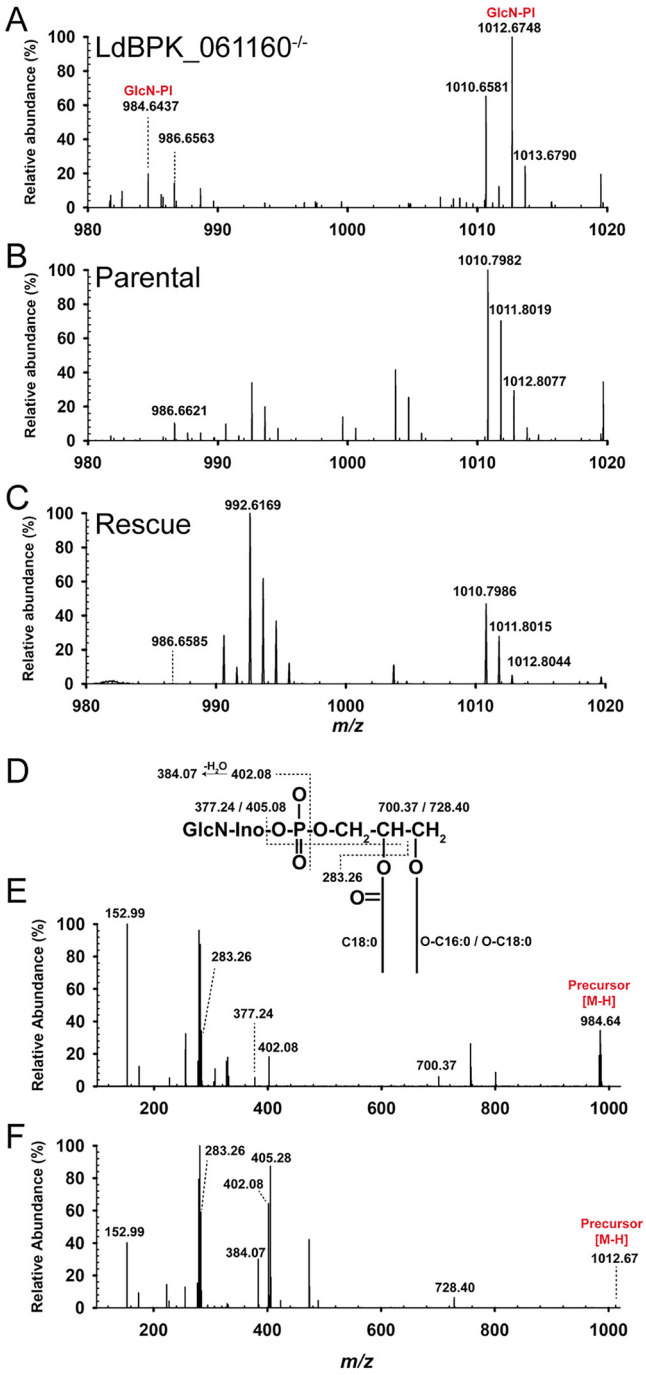

FIG 2 Disruptive targeting of *LdBPK_061160* causes an accumulation of the metabolite GlcN-PI demonstrating its requirement for GPI-mannosyltransferase I activity. Negative-ion electrospray mass spectrometry (ES-MS) spectra of lipid extracts from LdBPK_061160$^{-/-}$ (A), parental strain (B), and rescued null (C) showing the selective accumulation of the GlcN-PI precursor ions (red). (D) Schematic showing ES-MS^2 product ions of the GlcN-PI precursor ions. The ES-MS^2 HCD (high-energy C-trap dissociation) product ion spectra for the $[M - H]^-$ precursor ion at *m/z* 984.64 (E) and at *m/z* 1,012.67 (F) are shown. The difference between the precursors identified at *m/z* 984.64 (E) and 1,012.67 (F) was due to the length of the alkyl chain attached at position *sn-1* containing either $C_{16:0}$ (E) or $C_{18:0}$ (F). The product ion assignments for GlcN-PI species are indicated in panel D. The ion at *m/z* 402.08 representing [GlcN-*myo*-inositol-1,2-cyclic phosphate]$^-$ and its dehydration product at *m/z* 384.07 are characteristic of negative GlcN-PI product ion spectra. The ions at *m/z* 152.99 and 283.26 are [glycerol-cyclic phosphate]$^-$ and $[CH_3(CH_2)_{16}COO]^-$, respectively. The neutral loss of $C_{18:0}/(CH_3(CH_2)_{16}COO)^-$ is represented by ions at *m/z* 700.37 (E) and 728.40 (F), whereas the neutral loss of $C_{18:0}/(CH_3(CH_2)_{16}COO)^-$ and GlcN-inositol is represented by ions at *m/z* 377.24 (E) and 405.28 (F). The complete lipid profiles observed in negative-ion mode are shown in Fig. S1.

$C_{18:0}$). Upon higher-energy C-trap dissociation (HCD) fragmentation in MS^2, both $[M - H]^-$ ions at *m/z* 984.64 and 1,012.67 produced an intense ion at *m/z* 402.08 (Fig. 2D to F) which corresponded to GlcN-*myo*-inositol-1,2-cyclic phosphate which is a characteristic negative product ion for GlcN-PI in ES-MS^2. The alkylacyl based PI lipid species identified here are comparable to the previously reported GPI anchor lipid compositions in *Leishmania* (29–32). Because GlcN-PI species were undetectable in parental cells and mutant cells constitutively overexpressing *LdBPK_061160*, we conclude that the accumulation of GlcN-PI species in the mutant is caused by absence of *LdBPK_061160*. These data are consistent with mutant parasites lacking either a functional GPI-mannosyltransferase I (GPI-MT-I) complex or a flippase enzyme that transfers GlcN-PI from the cytosolic-facing leaflet of the lipid bilayer to the exoplasmic leaflet of the ER where the GPI-MT-I enzyme complex is localized.

The negative-ion ES-MS also identified the abundances of other major lipid species, including inositol phosphorylceramide (IPC), and phosphatidylinositol (PI) lipids, which were relatively unchanged in *LdBPK_061160*$^{-/-}$ parasites compared to the parental and genetically rescued lines (Fig. S1). In ES-MS^2, IPC and PI-based lipid species produced strong product ions at *m/z* 241 and *m/z* 259 corresponding to inositol-1,2-cyclic phosphate and inositol-monophosphate which are characteristic product ions of IPC and PI-based lipids in negative-ion mass spectrometry (data not shown). The lipid species identified here corroborate with previously reported lipid species in *Leishmania* (33, 34).

***LdBPK_061160* is the *PBN1* orthologue in *L. donovani*.** The mass spectrometry data alone were unable to distinguish whether *LdBPK_061160* functioned as an ER-localized flippase, or a component of the GPI-MT I complex. To distinguish between these possibilities, we first analyzed the structural architectures of the two classes of protein. While the identity of the ER-localized phospholipid flippase responsible for transferring GlcN-PI from the cytosolic face of the ER to the luminal face has yet to be elucidated (even with the advances in genome-wide CRISPR knockout screens [35]), there have been multiple enzymes identified from other organelles and organisms with reported phospholipid flipping activity (36–39). Sequence analysis of these phospholipid flipping enzymes reveal that they contain multiple (typically 4 to 10) transmembrane-spanning regions, whereas the protein architectures of PBN1 and PIG-X are more typical of a type I membrane protein with an N-terminal signal peptide and a single C-terminal transmembrane-spanning region (Fig. 3A). Based on this analysis, we concluded that the protein architecture of LdBPK_061160 is not consistent with a flippase enzyme.

To experimentally demonstrate that LdBPK_061160 is a PBN1 homolog, we attempted to rescue the loss of cell surface GPI-anchored molecules in the mutant parasite by the ectopic overexpression of the well-characterized human GPI-MT I enzymes. In agreement with previous studies, overexpression of human *PIG-X* or *PIG-M* alone was not individually capable of restoring the functional GPI pathway in the *LdBPK_061160* mutant; however, coexpression of both PIG-X and PIG-M restored staining of the GPI-anchored protein GP63 to the promastigote cell surface (Fig. 3B). Together, these data confirm that *LdBPK_061160* functions as the *Leishmania donovani* PBN1 homolog, and we therefore renamed this gene *LdPBN1*, in keeping with naming traditions for the trypanosomatid parasites.

One of the reasons that LdBPK_61160 had not previously been identified as a PIG-X/PBN1 orthologue is that the orthologues from different species vary significantly in size and have only low levels of sequence similarity. Consequently, simple sequence conservation had failed to identify the PIG-X/PBN1 homolog present in the related parasites *T. brucei* and *Trypanosoma cruzi*, which are the etiological agents of sleeping sickness and Chagas's disease, respectively. Because of greater sequence conservation among trypanosomatidae parasites, we were able to identify candidate PBN1 orthologues in all trypanosomatid species by sequence matching to LdBPK_61160 (Table S1 and Fig. S2). To establish whether these candidates were indeed functional orthologues, we asked whether the *T. cruzi* orthologue from the strain Silvio X10-7 (Contig ADWP02007247; nucleotides 5233.6071; 35% amino acid identity; referred to here as

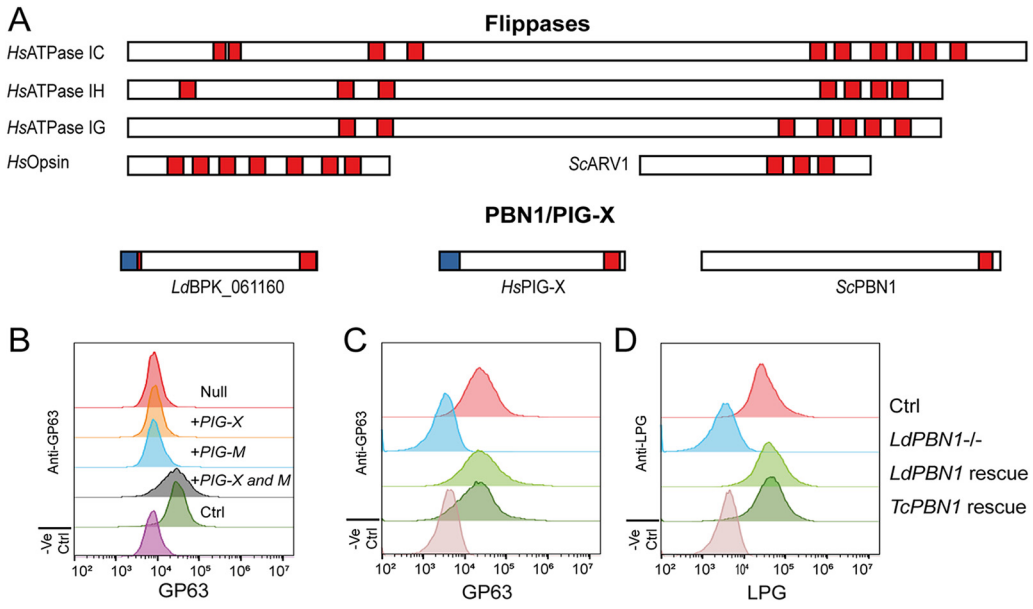

FIG 3 LdBPK_061160 is the *L. donovani* PBN1 orthologue. (A) Comparison of the protein sequence architecture of LdBPK_061160 with proteins of known flippase activity and the human and yeast PIG-X/PBN1 proteins. Note that LdBPK_061160 shares structural features with the PIG-X/PBN1 proteins and not the flippases. Predicted signal peptides are in blue, and transmembrane regions are in red. (B) Overexpression of the genes encoding *Homo sapiens* PIG-X and PIG-M in LdBPK_061160 mutants restores presence of GPI-anchored proteins at the cell surface. Histograms show cell surface staining of the GPI-anchored GP63 protein in LdBPK_061160 mutants overexpressing human genes encoding PIG-X, PIG-M, or both using a FITC-conjugated anti-GP63 monoclonal antibody by fluorescence-activated cell sorting (FACS). (C and D) Experimental identification of the PBN1 orthologue in *T. cruzi*. LdPBN1 mutants that lack surface expression of the GPI-anchored cell surface molecules GP63 and LPG were compared to the parental line and were genetically complemented with the gene encoding *T. cruzi* PBN1 (*TcPBN1*) (Contig ADWP02007247; nucleotides 5233.6071) or *LdPBN1* as a positive control. Levels of cell surface GP63 (C) and LPG (D) were quantified by staining parasites with monoclonal antibodies and flow cytometry. Results of one representative experiment of three are shown.

TcPBN1) could genetically complement the *LdPBN1* null mutant (Fig. S3). Overexpression of *TcPBN1* restored surface presentation of both GP63 and LPG to the same extent as the *LdPBN1* control, demonstrating that it is also a functional PBN1 (Fig. 3C and D).

LdPBN1 is essential for host infection. We next asked whether LdPBN1 mutants, which are viable *in vitro*, were able to establish an infection in a mammalian host. We used the LV9 strain of *L. donovani*, which stably expresses the firefly luciferase transgene, which permitted the longitudinal quantification of *in vivo* infection parameters using bioluminescent imaging (40). Using this model, parasites initially infect the liver and multiply to a peak at 2 weeks postinfection before they are gradually cleared and the focus of infection subsequently shifts to the spleen (Fig. 4A). Mice were inoculated intravenously with stationary-phase promastigotes from the bioluminescent parental strain, an LdPBN1-null mutant, and "rescued" mutants that constitutively expressed ectopic *LdPBN1*. As expected, we observed that mice infected with the parental strain showed robust infections that localized to the liver as early as day 3 postinfection (Fig. 4B and C), and which gradually progressed to the spleen (Fig. 4D). By contrast, *LdPBN1*$^{-/-}$ mutants failed to establish any detectable infection, with mice exhibiting only background levels of bioluminescence after 3 days (Fig. 4B and C). This effect could be rescued in the mutants by exogenous *LdPBN1*, confirming the causality of this gene (Fig. 4B and C). The inability of the *LdPBN1*$^{-/-}$ mutant to infect mice was reproducible showing the presence of a bioluminescent signal detected in the liver at 4 h postinfection which was reduced to background levels by day 3 (Fig. 4E), confirming that the mice challenged with an infectious dose were capable of rapidly controlling the infection. To determine if mutant parasites could persist below the limits of detection, we attempted to recover parasites from the spleens of infected mice by culturing

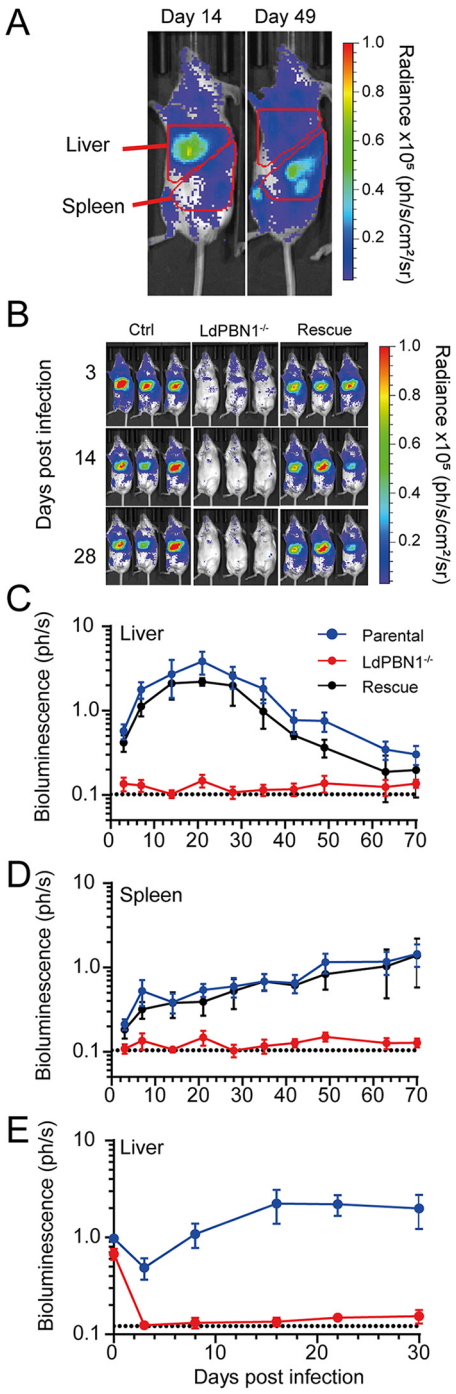

FIG 4 *L. donovani* PBN1 is essential for host infection. (A) Diagram showing examples of how infected animals were regionally gated to quantify infection load using bioluminescence imaging of the liver and the area corresponding to both the spleen and inguinal lymph node. (B) Groups of five mice were inoculated with stationary-phase promastigotes from parental (Ctrl), *PBN1*$^{-/-}$, and *PBN1*$^{-/-}$ parasites transfected with a *PBN1* expression rescue plasmid (rescue), and infections were longitudinally monitored by bioluminescence imaging. Quantification of liver (C) and spleen (D) bioluminescent signals from parental control parasites (blue), PBN1-deficient (red) and PBN1-deficient parasites rescued by overexpression of the PBN1 (black). The units of bioluminescence are 1×10^6 photons per second. Data are means and standard deviations (SD) ($n = 5$). Dotted line represents the average background bioluminescence from five unchallenged mice from a separate experiment measured over 77 days. Quantification of PBN1$^{-/-}$ infection between 4 h to 30 days postinfection in the liver (E). Bioluminescence is reported as 1×10^6 photons per second, and the data are from a single experiment where the group size was 5.

homogenates from isolated spleens. No *LdPBN1*$^{-/-}$ parasites were recovered despite readily recovering viable parasites from mice infected with parasites with a functional copy of *LdPBN1*, suggesting that GPI-anchored surface molecules are required for infection of mice.

Exposure to *LdPBN1*-deficient parasites elicits protection against the development of visceral leishmaniasis. Because the *LdPBN1*$^{-/-}$ mutant parasites were viable *in vitro* but incapable of establishing an infection *in vivo*, we asked whether they could be used as a genetically attenuated live parasite vaccine. We first determined if the mice inoculated with the *LdPBN1*$^{-/-}$ mutant parasites elicited a humoral immune response to the *LdPBN1*$^{-/-}$ mutant parasites by quantifying the ability of sera from infected mice to opsonize the cell surface of live promastigotes. Mice infected with either the parental *L. donovani* strain or the *LdPBN1*$^{-/-}$ mutant were able to generate a robust immune response at 14 days (Fig. 5A), with a further ~1.5-fold increase observed at 77 days postinfection (Fig. 5B). Despite the rapid clearance of the parasite, the titer of antibodies elicited by the *LdPBN1*$^{-/-}$ mutant recognizing the parasite cell surface was remarkably only fractionally lower than the parental line (Fig. 5A and B).

We next investigated if this host-elicited immune response against parasites that lack GPI-anchored cell surface molecules was capable of preventing or controlling an infection with a virulent strain. A pilot group of five mice that had been inoculated with *LdPBN1*$^{-/-}$ mutant *L. donovani* parasites for 12 weeks were segregated into two groups. Three mice were infected with the virulent bioluminescent parental strain, while the remaining two mice were left unchallenged to monitor any possible recrudescence that would confound our analysis. We observed that the three mice that had been preexposed to *LdPBN1*$^{-/-}$ mutant parasites could control the peak in liver bioluminescence, and the infection did not progress to the spleen (Fig. 5C and D). These findings were replicated using a larger cohort of 10 mice but with a reduced time between the initial inoculation and challenge. We observed that although immunized mice had a higher liver burden than their nonimmunized counterparts at 4 h postinfection (Fig. 5E), possibly due to antibody-dependent enhancement of infection, they were able to robustly control the initial infection in the liver. The immunized mice also showed significant levels of protection in the spleen between 28 and 56 days before the naive mice naturally resolved their infection after 60 days (Fig. 5F). Together, these results confirm that mice exposed to *L. donovani* lacking major classes of cell surface molecules are able to elicit a protective effect against the uncontrolled development of visceral leishmaniasis.

DISCUSSION

We have shown here that *LdBPK_061160* is the functional PBN1 homolog in *Leishmania donovani* parasites which is a necessary component of the glycosylphosphatidylinositol-mannosyltransferase I enzyme complex that performs an essential step in the GPI anchor-biosynthetic pathway. Although GPI anchors are present in all known eukaryotes, some components, including PIG-X/PBN1, show significant variation in sequence conservation, making them difficult to identify by sequence searching alone (25, 26).

Using functional complementation to restore GPI-MT I activity, we confirmed the role of *LdPBN1* by coexpression of both human *PIG-X* and *PIG-M* in LdBPK_061160-deficient parasites, and we were also able to identify, through sequence similarity, the PBN1 gene in *T. cruzi* and, by orthology, the same gene across all trypanosomatid species. This was recently confirmed by another group, who reported the identification and characterization of *Tb*PBN1 while revisions were being made to our manuscript (41). Remarkably, the sequence identity between *L. donovani* and *T. cruzi* PBN1 is just 35%, raising the question of what the minimal PBN1 sequence requirements are for stabilizing the GPI14 protein and complementing GPI-MT I function. It is known that the human and yeast gene products share only 19% amino acid identity and are functionally incompatible (Fig. S4), while the rat PIG-X homolog, which is 78% identical to the human protein, is capable of supporting the growth of yeast expressing *Hs*PIG-M, albeit at a significantly reduced rate (21, 26). While this confirms that cross-species

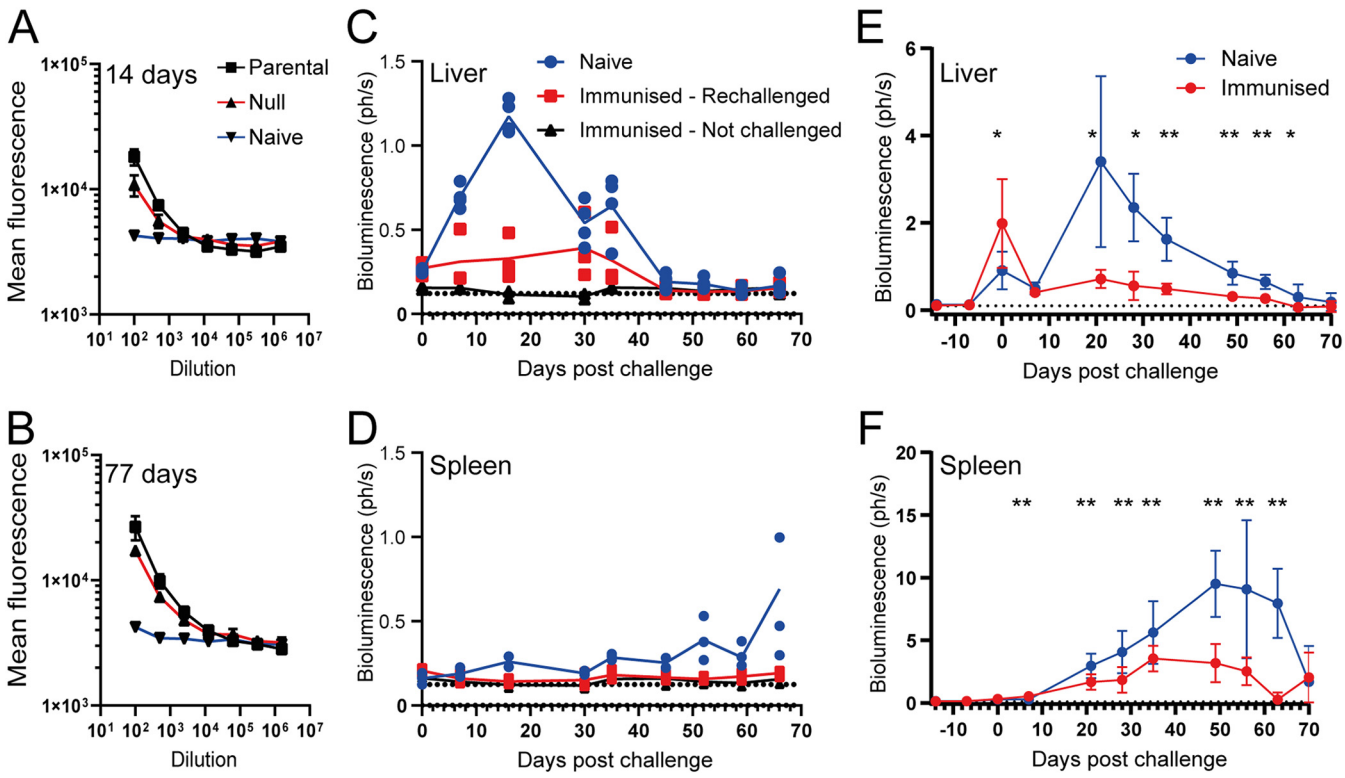

FIG 5 Inoculation with the LdPBN1 mutant is capable of eliciting a robust humoral immune response that offers significant protection against reinfection. Serum harvested from BALB/c mice that had been inoculated with either parental *L. donovani* parasites (black line) or PBN1$^{-/-}$ parasites (red line) for 14 (A) and 77 (B) days was diluted and used to stain live promastigotes by fluorescence-activated cell sorting, and results were compared to those for control mouse sera (blue line). (C to F) Inoculation with PBN1$^{-/-}$ parasites elicits protection against subsequent *L. donovani* infection. (C) Mice inoculated with the *L. donovani* PBN1$^{-/-}$ mutant were rested for 84 days before being infected with the bioluminescent virulent parental *L. donovani* strain, and the parasitemia was quantified in the livers (C) and spleens (D) of infected animals (red line, $n = 3$). Two mice were left uninfected to control for the possibility of recrudescence (black line), and four naive mice were infected as a positive infection control (blue line). (E and F) A group of 10 mice were inoculated with PBN1$^{-/-}$ mutant parasites and rested for 8 weeks prior to reinfection with the parental *L. donovani* strain and parasitemia quantified by bioluminescence in the liver (E) and spleen (F). Significantly different levels of parasitemia were assigned using a two-tailed Student's *t* test. *, $P < 0.05$, and **, $P < 0.001$, compared to a control group of 10 unimmunized mice. Data are from a single experiment, and bioluminescence is reported as 1×10^6 photons per second.

complementation of function is possible, there cannot be too much phylogenetic separation, because the orthologue of GPI14 from *Plasmodium falciparum* or *T. brucei* was incapable of restoring growth in GPI14-disrupted yeast (26). The inability of orthologues to complement loss of function across species is not uncommon for proteins where the sequence similarity is low. Analysis of human genes able to complement the loss of essential yeast genes reveals that they are typically shorter and have a higher sequence identity (42). In addition, they were less likely to be a component of a macromolecular complex and predicted to have fewer physical interactions. These observations could generally explain the limited ability to rescue of GPI-MT I activity through overexpression of homologs from more distantly separated ancestors. One possibility is that the functional context of human PIG-X differs from that of LdPBN1, and indeed, PIG-X is known to interact with two other proteins, RCN1 and RCN2 (43).

To demonstrate that *LdBPK_061160* was required for activity of the GPI-MT I complex, we showed that lipid extracts from the mutant parasites accumulated GlcN-PI, the precursor substrate for GPI-MT I. Interestingly, in comparison to the lipid extracts analyzed from *T. brucei* lacking the enzyme from the preceding step in the biosynthetic pathway (GlcNAc-PI de-N-acetylase, which is encoded by GPI12 and which converts GlcNAc-PI to GlcN-PI), a much smaller amount of the precursor lipid appears to accumulate (16). This could be an artifact in the extraction or analysis, or it could be that GlcN-PI exerts product inhibition on the GlcNAc-PI de-N-acetylase, limiting the accumulation of GlcN-PI, or that GlcN-PI is rapidly metabolized/catabolized in the absence of GPI-MT I activity.

Our initial interest in *LdBPK_061160* was as a possible cell surface vaccine target because it has primary sequence features that are compatible with it being an antibody-accessible cell surface membrane protein; however, our findings demonstrate that it is more likely to be localized to the intracellular endoplasmic reticulum membrane, where GPI-MT I activity is localized (44). It may, however, be possible to interfere with the interaction between PBN1 and GPI14 using rationally designed small molecules (45). We have shown that inhibiting the GPI biosynthesis pathway in *L. donovani* would affect parasite viability *in vivo*, and the significant protein sequence diversity between the parasite and mammalian proteins suggests that a drug could be designed that is specific for the parasite and lacks unwanted toxicity. This would be facilitated by characterizing the molecular details of the GPI14/PBN1 interaction interface. It is known that in the absence of PIG-X, the abundance of the catalytic subunit PIG-M is greatly reduced, indicating that the role of PBN1/PIG-X is as a stabilizing cofactor and/or molecular chaperone (21). This conclusion is further supported by an observed increase in the unfolded protein response in yeast in the absence of PBN1 (46), and chaperones have already been identified to be potential drug targets for diseases caused by protozoan parasites (47, 48).

The functional consequences of disrupting GPI-MT I in *L. donovani* are comparable with studies characterizing other mutants of the GPI anchor-biosynthetic enzymes in related parasites, including the observed increased adhesion phenotype (16, 17, 49, 50). Also, assessment of genes involved in mannose activation in *Leishmania mexicana* generally shows a requirement for phosphomannose mutase (51), GDP-mannose pyrophosphorylase (50, 52), for virulence, but not dolicholphosphate-mannose synthase (51). This is in contrast to our observations that the absence of multiple GPI-anchored surface molecule classes appears to affect the virulence of the parasites *in vivo*, as individually, parasites with targeted loss of LPG (53) or GPI-anchored proteins (54) are still able to infect mice. In the related parasite *T. brucei*, GPI-anchored proteins are necessary for cell survival in the bloodstream but not procyclic forms (55), and the underlying reason for this difference has yet to be fully elucidated, but it could plausibly be due to loss of the transferrin receptor, which is GPI anchored in *T. brucei* and essential for viability of bloodstream-form parasites (23, 56). It may be possible to address this by creating a non-GPI-anchored form of the transferrin receptor (57). Procyclic forms of *T. brucei* are thought to acquire iron from ferric complexes via a reductive mechanism (58), and consistent with this, *Leishmania* parasites acquire iron from their medium via a non-GPI anchor-mediated mechanism (59, 60), possibly explaining the discrepancies in observed lethalities between these parasites.

Finally, there is evidence that this mutant may have the potential to be exploited as a genetically attenuated live vaccine due to the significant levels of protection observed in both the liver and spleen. However, further investigations are needed to determine if this would be protective in the hamster model (61) or, alternatively, if this mutant would also provide protection against cutaneous disease (62). Despite a strong humoral response elicited by infection with the mutant, it remains to be determined if parasites lacking major components of its glycocalyx are capable of eliciting antibodies that recognize a broader range of surface proteins or protein epitopes. Our study adds another potential candidate to the list of candidates for an attenuated vaccine for the treatment of leishmaniasis, which currently includes the biopterin transporter (63), KHARON1 (64), p27 (65), and centrin. The centrin-null mutant has demonstrated protection against infection with a cutaneous-illness-causing strain (66) in addition to eliciting a protective response when it is replaced in a visceral-illness-causing species (67). Our findings here could therefore contribute to the development of a novel vaccine that could help limit or reduce the impact of this deadly infectious parasitic disease.

MATERIALS AND METHODS

Ethics statement. All animal experiments were performed under United Kingdom Home Office regulations (license numbers P98FFE489 and PD3DA8D1F) and European directive 2010/63/EU. Research was ethically approved by the local Sanger Institute Animal Welfare and Ethical Review Board. Mice

TABLE 1 Primers used to amplify ORFs for overexpression

Primer	Sequence
*LdBPK_061160*_F	CTAGGCTAGCATGTCGCGCGTAGTCGTGATG
*LdBPK_061160*_R	CTACTCTCGAGCTAACGAATAGCGAGGATAACGA
*TcPBN1*_F	CTAGGCTAGCATGATGCCTCTTTGTGTTTCTCC
*TcPBN1*_R	CTACTCTCGAGCTAAACACGCAGCAGCGAAA
*HsPIGX*_F	ATCTTAGCTAGCATGGCGGCTCGGGTGGCG
*HsPIGX*_R	ATCTTACTCGAGTTATAGGGAAAAATGGCCATATTTGAAAACTGCTACAAGGATCAATGTAG
*HsPIGM*_F	AATCACTAGATCTCTCGAGATGGGCTCCACCAAGCACTGGGG
*HsPIGM*_R	ATCTTAAGATCTCTAGTCATATTTGATTCTCTCTGTCAGGGGTTCTTCTTTGTAATGG

were maintained under a 12-h light/dark cycle at a temperature of 19 to 24°C and humidity between 40% and 65%. The animals used were 6- to 8-week-old female *Mus musculus* strain BALB/c obtained from a breeding colony at the Wellcome Sanger Institute.

***L. donovani* cell culture.** Parasites were maintained as described previously (40) in continuous culture supplemented with or without nourseothricin, hygromycin, blasticidin, puromycin, or phleomycin at 100, 50, 25, 15, and 20 μg mL^{-1} as appropriate. Single-cell suspensions were obtained by detaching parasites through vigorous shaking and passing through a 10-μm cell strainer (pluriStrainer).

CRISPR-Cas9-mediated deletion of *LdBPK_061160* and genetic rescue. The *LdBPK_061160* gene was targeted by CRISPR-Cas9 mediated deletion using the approach previously described (68) with the primers documented in Table 1, and correct targeting by CRISPR-Cas9 was assessed by PCR. The open reading frames (ORFs) of *LdBPK_061160* and *T. cruzi* were amplified using primers designed against *TcCLB.508173.240* from *T. cruzi* Silvio X10/7 genomic DNA, with primers containing engineered NheI and XhoI endonuclease restriction sites (Table 1). The purified PCR products and the plasmid PTBLE were digested with NheI and XhoI and the ORFs ligated into the linearized plasmid yielding PTBLE-*LdBK_061160* and PTBLE-*TcPBN1*, respectively. SwaI-digested plasmids were electroporated into mid-log-phase promastigotes using an Amaxa Nucleofector 2b device as previously described (68). Transgenic parasites were selected by the addition of phleomycin (20 μg mL^{-1}) until parasites in a no-plasmid control transfection had died. cDNAs encoding *HsPIG-X* and *HsPIG-M* were amplified using specific primers (Table 1) from plasmids carrying genes NM_017861.3 and NM_145167.2 (Sino Biological), and the PCR products were cloned into PTBLE and pRIB expression plasmids using standard restriction enzyme methods (69).

Mouse infections and serum collection. Groups of five female BALB/c mice were infected with 1×10^8 stationary-phase promastigotes via the intravenous route as previously described (40). Serum was collected from infected mice through tail bleed and clotted by incubating at 37°C for 30 min, prior to centrifugation at 20,000 $\times$ *g* for 15 min.

Flow cytometry and microscopy. Mid-log promastigotes were harvested by centrifugation at 800 $\times$ *g* for 5 min at 23°C and resuspended at a concentration of 1.1×10^8 mL^{-1} in ice-cold phosphate-buffered saline (PBS). A total of 1×10^7 parasites were stained with or without mouse anti-GP63–FITC (fluorescein isothiocyanate) (clone 96/26, used at a 1/100 dilution), mouse anti-LPG (clone CA7AE, used at a 1/10,000 dilution), or mouse anti-*L. donovani* (polyclonal, used at a 1/1,000 dilution) for 1 h at 4°C. Parasites were washed three times in PBS and stained with goat anti-mouse IgG–Alexa Fluor 488 (1/1,000 dilution), goat anti-mouse IgG–Alexa Fluor 633 (1/1,000 dilution), or rabbit anti-IgM–Alexa Fluor 633 (1/1,000 dilution) for 1 h at 4°C prior to washing in PBS three times. Washed parasites were biologically inactivated with a 2% formalin solution buffered in PBS for 15 min at 23°C, and buffer was exchanged into PBS for analysis on a CytoFLEX S flow cytometer (Beckman Coulter). A total of 10,000 events were collected and analyzed in FlowJo (v10.6.1). Fluorescent images were acquired on an Axio Vert.A1 equipped with an AxioCam ERc 5s, with a Colibri 7 LED light source using appropriate filter sets and a 40$\times$ or 100$\times$ objective. Exposure times were standardized and the monochromatic images processed in Fiji (70).

Metabolite identification from lipid extracts by mass spectrometry. Promastigotes of parental, *LdBPK_061160* null mutant and genetically rescued cells of *L. donovani* (5×10^8 of each) in mid-logarithmic growth were harvested by centrifugation and washed three times with PBS. The lipids were extracted as previously reported (16). Briefly, the cells were extracted with chloroform-methanol-water (10:10:3 [vol/vol/vol]) overnight at 4°C and sonicated for 15 min in a sonicating water bath. The extract was centrifuged for 5 min at full speed, and the supernatant was dried under a nitrogen stream in a fresh tube. The dried extract was subjected to butan-1-ol–water (1:1 [vol/vol], 200 μL each) partition, and the aqueous phase was partitioned twice with 0.2 mL water-saturated butan-1-ol. The butan-1-ol phases were pooled and backwashed three times with 0.4 mL water saturated with butan-1-ol. The washed butan-1-ol phases were dried under a nitrogen stream and dissolved in 50 μL chloroform-methanol-water (10:10:3) for electrospray-ionization mass spectrometry (ES-MS) analysis. Five microliters of sample was infused into the Orbitrap Fusion Tribrid mass spectrometer (Thermo Scientific) using static infusion nanoflow probe tips (M956232AD1-S; Waters). ES-MS and ES-MS^2 analysis were performed in negative-ion mode using negative-ion spray voltage as 0.7 kV and the ion transfer tube temperature was 275°C. Collision-induced dissociation (CID) and high-energy C-trap dissociation (HCD) were used for ES-MS^2 fragmentation, using 30 to 45% collision energy.

SUPPLEMENTAL MATERIAL

Supplemental material is available online only.

FIG S1, PDF file, 0.2 MB.

FIG S2, PDF file, 0.3 MB.

FIG S3, PDF file, 0.2 MB.

FIG S4, PDF file, 0.3 MB.

TABLE S1, PDF file, 0.2 MB.

ACKNOWLEDGMENTS

We thank Eva Gluenz (University of Glasgow) for providing us with the Cas9 plasmids, Jeremy Mottram (University of York) for providing the pRIB plasmid, Mary Wilson (University of Iowa) for the *L. donovani* mCherry/LUC parasites and Susan Wylie (University of Dundee) for providing the *T. cruzi* gDNA. We also thank the cytometry core facility at the Sanger Institute.

A.R., G.J.W., M.A.J.F., S.C., and R.N. participated in the design of this study. A.R., S.C., C.B., K.H., and R.N. collected the data, and all authors were involved with the analysis. All authors contributed to the manuscript writing and editing.

This work was funded by the Wellcome Trust (grant 206194). R.N. and M.A.J.F. were supported by a Wellcome Investigator Award to M.A.J.F. (101842/Z/13/Z).

We declare that we have no conflicts of interest with the contents of this article.

REFERENCES

1. WHO. 2021. Leishmaniasis fact sheet. WHO fact sheet.
2. WHO. 2016. Leishmaniasis in high-burden countries: an epidemiological update based on data reported in 2014. Wkly Epidemiol Rec 91:287–296.
3. Lindoso JAL, Costa JML, Queiroz IT, Goto H. 2012. Review of the current treatments for leishmaniases. Res Rep Trop Med 3:69–77. https://doi.org/10.2147/RRTM.S24764.
4. Srivastava S, Mishra J, Gupta AK, Singh A, Shankar P, Singh S. 2017. Laboratory confirmed miltefosine resistant cases of visceral leishmaniasis from India. Parasit Vectors 10:49. https://doi.org/10.1186/s13071-017-1969-z.
5. Croft SL, Sundar S, Fairlamb AH. 2006. Drug resistance in leishmaniasis. Clin Microbiol Rev 19:111–126. https://doi.org/10.1128/CMR.19.1.111-126.2006.
6. Deep DK, Singh R, Bhandari V, Verma A, Sharma V, Wajid S, Sundar S, Ramesh V, Dujardin JC, Salotra P. 2017. Increased miltefosine tolerance in clinical isolates of *Leishmania donovani* is associated with reduced drug accumulation, increased infectivity and resistance to oxidative stress. PLoS Negl Trop Dis 11:e0005641. https://doi.org/10.1371/journal.pntd.0005641.
7. Wyllie S, Thomas M, Patterson S, Crouch S, De Rycker M, Lowe R, Gresham S, Urbaniak MD, Otto TD, Stojanovski L, Simeons FRC, Manthri S, MacLean LM, Zuccotto F, Homeyer N, Pflaumer H, Boesche M, Sastry L, Connolly P, Albrecht S, Berriman M, Drewes G, Gray DW, Ghidelli-Disse S, Dixon S, Fiandor JM, Wyatt PG, Ferguson MAJ, Fairlamb AH, Miles TJ, Read KD, Gilbert IH. 2018. Cyclin-dependent kinase 12 is a drug target for visceral leishmaniasis. Nature 560:192–197. https://doi.org/10.1038/s41586-018-0356-z.
8. Wyllie S, Patterson S, Stojanovski L, Simeons FRC, Norval S, Kime R, Read KD, Fairlamb AH. 2012. The anti-trypanosome drug fexinidazole shows potential for treating visceral leishmaniasis. Sci Transl Med 4:119re1. https://doi.org/10.1126/scitranslmed.3003326.
9. Patterson S, Wyllie S, Stojanovski L, Perry MR, Simeons FRC, Norval S, Osuna-Cabello M, De Rycker M, Read KD, Fairlamb AH. 2013. The R enantiomer of the antitubercular drug PA-824 as a potential oral treatment for visceral Leishmaniasis. Antimicrob Agents Chemother 57:4699–4706. https://doi.org/10.1128/AAC.00722-13.
10. McConville MJ, Ferguson MA. 1993. The structure, biosynthesis and function of glycosylated phosphatidylinositols in the parasitic protozoa and higher eukaryotes. Biochem J 294:305–324. https://doi.org/10.1042/bj2940305.
11. Ferguson MAJ, Hart GW, Kinoshita T. 2015. Glycosylphosphatidylinositol anchors, p 137–150. *In* Varki A, Cummings RD, Esko JD, Stanley P, Hart GW, Aebi M, Darvill AG, Kinoshita T, Packer NH, Prestegard JH, Schnaar RL, Seeberger PH (ed), Essentials of glycobiology. Cold Spring Harbor Press, Cold Spring Harbor, NY.
12. Ferguson MA, Homans SW, Dwek RA, Rademacher TW. 1988. Glycosylphosphatidylinositol moiety that anchors *Trypanosoma brucei* variant surface glycoprotein to the membrane. Science 239:753–759. https://doi.org/10.1126/science.3340856.
13. Horn D. 2014. Antigenic variation in African trypanosomes. Mol Biochem Parasitol 195:123–129. https://doi.org/10.1016/j.molbiopara.2014.05.001.
14. Turco SJ, Descoteaux A. 1992. The lipophosphoglycan of Leishmania parasites. Annu Rev Microbiol 46:65–94. https://doi.org/10.1146/annurev.mi.46.100192.000433.
15. Arango Duque G, Descoteaux A. 2015. Leishmania survival in the macrophage: where the ends justify the means. Curr Opin Microbiol 26:32–40. https://doi.org/10.1016/j.mib.2015.04.007.
16. Güther ML, Lee S, Tetley L, Acosta-Serrano A, Ferguson MA. 2006. GPI-anchored proteins and free GPI glycolipids of procyclic form *Trypanosoma brucei* are nonessential for growth, are required for colonization of the tsetse fly, and are not the only components of the surface coat. Mol Biol Cell 17:5265–5274. https://doi.org/10.1091/mbc.e06-08-0702.
17. Nagamune K, Nozaki T, Maeda Y, Ohishi K, Fukuma T, Hara T, Schwarz RT, Sütterlin C, Brun R, Riezman H, Kinoshita T. 2000. Critical roles of glycosylphosphatidylinositol for *Trypanosoma brucei*. Proc Natl Acad Sci U S A 97:10336–10341. https://doi.org/10.1073/pnas.180230697.
18. Masterson WJ, Doering TL, Hart GW, Englund PT. 1989. A novel pathway for glycan assembly: biosynthesis of the glycosyl-phosphatidylinositol anchor of the trypanosome variant surface glycoprotein. Cell 56:793–800. https://doi.org/10.1016/0092-8674(89)90684-3.
19. Pittet M, Conzelmann A. 2007. Biosynthesis and function of GPI proteins in the yeast *Saccharomyces cerevisiae*. Biochim Biophys Acta 1771:405–420. https://doi.org/10.1016/j.bbalip.2006.05.015.
20. Murakami Y, Siripanyapinyo U, Hong Y, Kang JY, Ishihara S, Nakakuma H, Maeda Y, Kinoshita T. 2003. PIG-W is critical for inositol acylation but not for flipping of glycosylphosphatidylinositol-anchor. Mol Biol Cell 14:4285–4295. https://doi.org/10.1091/mbc.e03-03-0193.
21. Ashida H, Hong Y, Murakami Y, Shishioh N, Sugimoto N, Kim YU, Maeda Y, Kinoshita T. 2005. Mammalian PIG-X and yeast Pbn1p are the essential components of glycosylphosphatidylinositol-mannosyltransferase I. Mol Biol Cell 16:1439–1448. https://doi.org/10.1091/mbc.e04-09-0802.
22. Güther ML, Ferguson MA. 1995. The role of inositol acylation and inositol deacylation in GPI biosynthesis in *Trypanosoma brucei*. EMBO J 14:3080–3093. https://doi.org/10.1002/j.1460-2075.1995.tb07311.x.
23. Ferguson MAJ. 2000. Glycosylphosphatidylinositol biosynthesis validated as a drug target for African sleeping sickness. Proc Natl Acad Sci U S A 97:10673–10675. https://doi.org/10.1073/pnas.97.20.10673.

24. Smith TK, Crossman A, Brimacombe JS, Ferguson MA. 2004. Chemical validation of GPI biosynthesis as a drug target against African sleeping sickness. EMBO J 23:4701–4708. https://doi.org/10.1038/sj.emboj.7600456.
25. Cardoso MS, Junqueira C, Trigueiro RC, Shams-Eldin H, Macedo CS, Araújo PR, Gomes DA, Martinelli PM, Kimmel J, Stahl P, Niehus S, Schwarz RT, Previato JO, Mendonça-Previato L, Gazzinelli RT, Teixeira SMR. 2013. Identification and functional analysis of *Trypanosoma cruzi* genes that encode proteins of the glycosylphosphatidylinositol biosynthetic pathway. PLoS Negl Trop Dis 7:e2369. https://doi.org/10.1371/journal.pntd.0002369.
26. Kim YU, Ashida H, Mori K, Maeda Y, Hong Y, Kinoshita T. 2007. Both mammalian PIG-M and PIG-X are required for growth of GPI14-disrupted yeast. J Biochem 142:123–129. https://doi.org/10.1093/jb/mvm113.
27. Schneider P, Ferguson MA, McConville MJ, Mehlert A, Homans SW, Bordier C. 1990. Structure of the glycosyl-phosphatidylinositol membrane anchor of the *Leishmania major* promastigote surface protease. J Biol Chem 265:16955–16964. https://doi.org/10.1016/S0021-9258(17)44853-8.
28. Puentes SM, Dwyer DM, Bates PA, Joiner KA. 1989. Binding and release of C3 from *Leishmania donovani* promastigotes during incubation in normal human serum. J Immunol 143:3743–3749.
29. McConville MJ, Mullin KA, Ilgoutz SC, Teasdale RD. 2002. Secretory pathway of trypanosomatid parasites. Microbiol Mol Biol Rev 66:122–154; table of contents. https://doi.org/10.1128/MMBR.66.1.122-154.2002.
30. Ralton JE, McConville MJ. 1998. Delineation of three pathways of glycosylphosphatidylinositol biosynthesis in *Leishmania mexicana*. Precursors from different pathways are assembled on distinct pools of phosphatidylinositol and undergo fatty acid remodeling. J Biol Chem 273:4245–4257. https://doi.org/10.1074/jbc.273.7.4245.
31. Ilgoutz SC, McConville MJ. 2001. Function and assembly of the Leishmania surface coat. Int J Parasitol 31:899–908. https://doi.org/10.1016/s0020-7519(01)00197-7.
32. Ferguson MA. 1997. The surface glycoconjugates of trypanosomatid parasites. Philos Trans R Soc Lond B Biol Sci 352:1295–1302. https://doi.org/10.1098/rstb.1997.0113.
33. Zufferey R, Allen S, Barron T, Sullivan DR, Denny PW, Almeida IC, Smith DF, Turco SJ, Ferguson MAJ, Beverley SM. 2003. Ether phospholipids and glycosylinositolphospholipids are not required for amastigote virulence or for inhibition of macrophage activation by *Leishmania major*. J Biol Chem 278:44708–44718. https://doi.org/10.1074/jbc.M308063200.
34. Denny PW, Goulding D, Ferguson MA, Smith DF. 2004. Sphingolipid-free Leishmania are defective in membrane trafficking, differentiation and infectivity. Mol Microbiol 52:313–327. https://doi.org/10.1111/j.1365-2958.2003.03975.x.
35. Sharma S, Bartholdson SJ, Couch ACM, Yusa K, Wright GJ. 2018. Genome-scale identification of cellular pathways required for cell surface recognition. Genome Res 28:1372–1382. https://doi.org/10.1101/gr.231183.117.
36. Kajiwara K, Watanabe R, Pichler H, Ihara K, Murakami S, Riezman H, Funato K. 2008. Yeast ARV1 is required for efficient delivery of an early GPI intermediate to the first mannosyltransferase during GPI assembly and controls lipid flow from the endoplasmic reticulum. Mol Biol Cell 19:2069–2082. https://doi.org/10.1091/mbc.e07-08-0740.
37. Menon AK, Watkins WE, Hrafnsdóttir S. 2000. Specific proteins are required to translocate phosphatidylcholine bidirectionally across the endoplasmic reticulum. Curr Biol 10:241–252. https://doi.org/10.1016/S0960-9822(00)00356-0.
38. Menon I, Huber T, Sanyal S, Banerjee S, Barré P, Canis S, Warren JD, Hwa J, Sakmar TP, Menon AK. 2011. Opsin is a phospholipid flippase. Curr Biol 21:149–153. https://doi.org/10.1016/j.cub.2010.12.031.
39. Andersen JP, Vestergaard AL, Mikkelsen SA, Mogensen LS, Chalat M, Molday RS. 2016. P4-ATPases as phospholipid flippases—structure, function, and enigmas. Front Physiol 7:275–275. https://doi.org/10.3389/fphys.2016.00275.
40. Ong HB, Clare S, Roberts AJ, Wilson ME, Wright GJ. 2020. Establishment, optimisation and quantitation of a bioluminescent murine infection model of visceral leishmaniasis for systematic vaccine screening. Sci Rep 10:4689. https://doi.org/10.1038/s41598-020-61662-3.
41. Cowton A, Bütikofer P, Häner R, Menon AK. 2022. Identification of TbPBN1 in Trypanosoma brucei reveals a conserved heterodimeric architecture for glycosylphosphatidylinositol-mannosyltransferase-I. Mol Microbiol 117:450–461. https://doi.org/10.1111/mmi.14859.
42. Hamza A, Tammpere E, Kofoed M, Keong C, Chiang J, Giaever G, Nislow C, Hieter P. 2015. Complementation of yeast genes with human genes as an experimental platform for functional testing of human genetic variants. Genetics 201:1263–1274. https://doi.org/10.1534/genetics.115.181099.
43. Nakakido M, Tamura K, Chung S, Ueda K, Fujii R, Kiyotani K, Nakamura Y. 2016. Phosphatidylinositol glycan anchor biosynthesis, class X containing complex promotes cancer cell proliferation through suppression of EHD2 and ZIC1, putative tumor suppressors. Int J Oncol 49:868–876. https://doi.org/10.3892/ijo.2016.3607.
44. Maeda Y, Watanabe R, Harris CL, Hong Y, Ohishi K, Kinoshita K, Kinoshita T. 2001. PIG-M transfers the first mannose to glycosylphosphatidylinositol on the lumenal side of the ER. EMBO J 20:250–261. https://doi.org/10.1093/emboj/20.1.250.
45. Lu H, Zhou Q, He J, Jiang Z, Peng C, Tong R, Shi J. 2020. Recent advances in the development of protein–protein interactions modulators: mechanisms and clinical trials. Signal Transduct Target Ther 5:213. https://doi.org/10.1038/s41392-020-00315-3.
46. Subramanian S, Woolford CA, Drill E, Lu M, Jones EW. 2006. Pbn1p: an essential endoplasmic reticulum membrane protein required for protein processing in the endoplasmic reticulum of budding yeast. Proc Natl Acad Sci U S A 103:939–944. https://doi.org/10.1073/pnas.0505570103.
47. Pallavi R, Roy N, Nageshan RK, Talukdar P, Pavithra SR, Reddy R, Venketesh S, Kumar R, Gupta AK, Singh RK, Yadav SC, Tatu U. 2010. Heat shock protein 90 as a drug target against protozoan infections: biochemical characterization of HSP90 from *Plasmodium falciparia* and *Trypanosoma evansi* and evaluation of its inhibitors as a candidate drug. J Biol Chem 285:37964–37975. https://doi.org/10.1074/jbc.M110.155317.
48. Murillo-Solano C, Dong C, Sanchez CG, Pizarro JC. 2017. Identification and characterization of the antiplasmodial activity of Hsp90 inhibitors. Malar J 16:292. https://doi.org/10.1186/s12936-017-1940-7.
49. Almani PGN, Sharifi I, Kazemi B, Babaei Z, Bandehpour M, Salari S, Dezaki ES, Tohidi F, Mohammadi MA. 2016. The role of GlcNAc-PI-de-N-acetylase gene by gene knockout through homologous recombination and its consequences on survival, growth and infectivity of *Leishmania major* in in vitro and in vivo conditions. Acta Trop 154:63–72. https://doi.org/10.1016/j.actatropica.2015.10.025.
50. Stewart J, Curtis J, Spurck TP, Ilg T, Garami A, Baldwin T, Courret N, McFadden GI, Davis A, Handman E. 2005. Characterisation of a *Leishmania mexicana* knockout lacking guanosine diphosphate-mannose pyrophosphorylase. Int J Parasitol 35:861–873. https://doi.org/10.1016/j.ijpara.2005.03.008.
51. Garami A, Mehlert A, Ilg T. 2001. Glycosylation defects and virulence phenotypes of *Leishmania mexicana* phosphomannomutase and dolichol-phosphate-mannose synthase gene deletion mutants. Mol Cell Biol 21:8168–8183. https://doi.org/10.1128/MCB.21.23.8168-8183.2001.
52. Garami A, Ilg T. 2001. Disruption of mannose activation in *Leishmania mexicana*: GDP-mannose pyrophosphorylase is required for virulence, but not for viability. EMBO J 20:3657–3666. https://doi.org/10.1093/emboj/20.14.3657.
53. Ilg T. 2000. Lipophosphoglycan is not required for infection of macrophages or mice by *Leishmania mexicana*. EMBO J 19:1953–1962. https://doi.org/10.1093/emboj/19.9.1953.
54. Ellis M, Sharma DK, Hilley JD, Coombs GH, Mottram JC. 2002. Processing and trafficking of *Leishmania mexicana* GP63. Analysis using GP18 mutants deficient in glycosylphosphatidylinositol protein anchoring. J Biol Chem 277:27968–27974. https://doi.org/10.1074/jbc.M202047200.
55. Lillico S, Field MC, Blundell P, Coombs GH, Mottram JC. 2003. Essential roles for GPI-anchored proteins in African trypanosomes revealed using mutants deficient in GPI8. Mol Biol Cell 14:1182–1194. https://doi.org/10.1091/mbc.e02-03-0167.
56. Tiengwe C, Muratore KA, Bangs JD. 2016. Surface proteins, ERAD and antigenic variation in *Trypanosoma brucei*. Cell Microbiol 18:1673–1688. https://doi.org/10.1111/cmi.12605.
57. Kabiri M, Steverding D. 2021. *Trypanosoma brucei* transferrin receptor: functional replacement of the GPI anchor with a transmembrane domain. Mol Biochem Parasitol 242:111361. https://doi.org/10.1016/j.molbiopara.2021.111361.
58. Mach J, Tachezy J, Sutak R. 2013. Efficient iron uptake via a reductive mechanism in procyclic *Trypanosoma brucei*. J Parasitology 99:363–364. https://doi.org/10.1645/GE-3237.1.
59. Miguel DC, Flannery AR, Mittra B, Andrews NW. 2013. Heme uptake mediated by LHR1 is essential for *Leishmania amazonensis* virulence. Infect Immun 81:3620–3626. https://doi.org/10.1128/IAI.00687-13.
60. Flannery AR, Renberg RL, Andrews NW. 2013. Pathways of iron acquisition and utilization in Leishmania. Curr Opin Microbiol 16:716–721. https://doi.org/10.1016/j.mib.2013.07.018.
61. Reimão JQ, Oliveira JC, Trinconi CT, Cotrim PC, Coelho AC, Uliana SR. 2015. Generation of luciferase-expressing *Leishmania infantum* chagasi and

assessment of miltefosine efficacy in infected hamsters through bioimaging. PLoS Negl Trop Dis 9:e0003556. https://doi.org/10.1371/journal.pntd.0003556.
62. Ashwin H, Sadlova J, Vojtkova B, Becvar T, Lypaczewski P, Schwartz E, Greensted E, Van Bocxlaer K, Pasin M, Lipinski KS, Parkash V, Matlashewski G, Layton AM, Lacey CJ, Jaffe CL, Volf P, Kaye PM. 2021. Characterization of a new *Leishmania major* strain for use in a controlled human infection model. Nat Commun 12:215. https://doi.org/10.1038/s41467-020-20569-3.
63. Papadopoulou B, Roy G, Breton M, Kündig C, Dumas C, Fillion I, Singh AK, Olivier M, Ouellette M. 2002. Reduced infectivity of a *Leishmania donovani* biopterin transporter genetic mutant and its use as an attenuated strain for vaccination. Infect Immun 70:62–68. https://doi.org/10.1128/IAI.70.1.62-68.2002.
64. Santi AMM, Lanza JS, Tunes LG, Fiuza JA, Roy G, Orfanó AS, de Carvalho AT, Frézard F, Barros ALBd, Murta SMF, do Monte-Neto RL. 2018. Growth arrested live-attenuated *Leishmania infantum* KHARON1 null mutants display cytokinesis defect and protective immunity in mice. Sci Rep 8:11627. https://doi.org/10.1038/s41598-018-30076-7.
65. Dey R, Dagur PK, Selvapandiyan A, McCoy JP, Salotra P, Duncan R, Nakhasi HL. 2013. Live attenuated *Leishmania donovani* p27 gene knockout parasites are nonpathogenic and elicit long-term protective immunity in BALB/c mice. J Immunol) 190:2138–2149. https://doi.org/10.4049/jimmunol.1202801.
66. Zhang W-W, Karmakar S, Gannavaram S, Dey R, Lypaczewski P, Ismail N, Siddiqui A, Simonyan V, Oliveira F, Coutinho-Abreu IV, DeSouza-Vieira T, Meneses C, Oristian J, Serafim TD, Musa A, Nakamura R, Saljoughian N, Volpedo G, Satoskar M, Satoskar S, Dagur PK, McCoy JP, Kamhawi S, Valenzuela JG, Hamano S, Satoskar AR, Matlashewski G, Nakhasi HL. 2020. A second generation leishmanization vaccine with a markerless attenuated *Leishmania major* strain using CRISPR gene editing. Nat Commun 11:3461. https://doi.org/10.1038/s41467-020-17154-z.
67. Bhattacharya P, Dey R, Dagur PK, Joshi AB, Ismail N, Gannavaram S, Debrabant A, Akue AD, KuKuruga MA, Selvapandiyan A, McCoy JP, Jr, Nakhasi HL. 2016. Live attenuated *Leishmania donovani* centrin knock out parasites generate non-inferior protective immune response in aged mice against visceral leishmaniasis. PLoS Negl Trop Dis 10:e0004963. https://doi.org/10.1371/journal.pntd.0004963.
68. Beneke T, Madden R, Makin L, Valli J, Sunter J, Gluenz E. 2017. A CRISPR Cas9 high-throughput genome editing toolkit for kinetoplastids. R Soc Open Sci 4:170095. https://doi.org/10.1098/rsos.170095.
69. Misslitz A, Mottram JC, Overath P, Aebischer T. 2000. Targeted integration into a rRNA locus results in uniform and high level expression of transgenes in Leishmania amastigotes. Mol Biochem Parasitol 107:251–261. https://doi.org/10.1016/s0166-6851(00)00195-x.
70. Schindelin J, Arganda-Carreras I, Frise E, Kaynig V, Longair M, Pietzsch T, Preibisch S, Rueden C, Saalfeld S, Schmid B, Tinevez J-Y, White DJ, Hartenstein V, Eliceiri K, Tomancak P, Cardona A. 2012. Fiji: an open-source platform for biological-image analysis. Nat Methods 9:676–682. https://doi.org/10.1038/nmeth.2019.